Electronic Supplementary Material (ESI) for ChemComm.

Supporting Information for

Lewis acid Mg^{2+}-doped cobalt phosphate nanosheets for enhanced electrocatalytic oxygen evolution reaction

Jing Qi,[a] Xinxin Shen,[a] Mingxing Chen,[a] Enbo Shangguan,[*a] Wei Zhang[*b] and Rui Cao[*b]

[a] School of Materials Science and Engineering, Henan Normal University, Xinxiang 453007, China

[b] Key Laboratory of Applied Surface and Colloid Chemistry, Ministry of Education, School of Chemistry and Chemical Engineering, Shaanxi Normal University, Xi'an 710119, China

[*] Correspondence to: zw@snnu.edu.cn; ruicao@snnu.edu.cn; shangguanenbo@163.com;

General materials

All chemicals, including $Co(NO_3)_2 \cdot 6H_2O$ (99.999%, Alfa), $(NH_4)_3PO_4 \cdot 3H_2O$ (98%, Tianli Chemical Reagent Co.), C_2H_5OH (99.5%, Sigma–Aldrich), KOH (98%, Sinopharm Chemicals), $MgCl_2 \cdot 6H_2O$ (98.0%, Sinopharm Chemicals) and Nafion (5 wt%, DuPont) were obtained from commercial suppliers and used without further purification. Milli-Q water of 18.2 MΩ·cm was used in all experiments.

Synthesis of NH_4CoPO_4 precursors

NH_4CoPO_4 nanosheets were synthesized by a simple coprecipitation method. First, $Co(NO_3)_2 \cdot 6H_2O$ (1 mmol) was added into 20 mL C_2H_5OH, and treated with ultrasound until dissolved. Afterward, $(NH_4)_3PO_4 \cdot 3H_2O$ (5 mmol) was dissolved in 20 mL DI water by ultrasonication. The above solution was dropped into cobalt alcohol solution under ultrasonic condition. The obtained precursors were washed several times with DI water and dried in an oven at 60 ^oC.

Synthesis of Mg-doped $Co_3(PO_4)_2$ nanosheets

NH_4CoPO_4 (20 mmol) precursors were first dispersed in 10 mL DI water by ultrasonic treatment, noted as solution A. $MgCl_2 \cdot 6H_2O$ (10 mmol) was dissolved in 10 mL DI water, noted as solution B. Solution B was added into solution A under magnetic stirring. The mixed suspension was subsequently stirred at 80 ^oC for 3 h. The pink powder was collected and washed by DI water thoroughly. Finally, the obtained product was dried at 60 ^oC overnight. The Mg-doped $Co_3(PO_4)_2$ materials with different Mg contents were synthesized by changing the amounts of $MgCl_2 \cdot 6H_2O$ to 5 and 20 mmol.

Synthesis of pure $Co_3(PO_4)_2$ nanosheets

$Co(NO_3)_2 \cdot 6H_2O$ (1 mmol) was added in 20 mL C_2H_5OH, and treated with ultrasound

until dissolved. Afterward, $(NH_4)_3PO_4 \cdot 3H_2O$ (1 mmol) was dissolved in 20 mL DI water by ultrasonication. The above solution was dropped on cobalt alcohol solution under ultrasonic condition. The obtained product was washed several times with DI water and dried in an oven at 60 ^oC.

Physical characterization

Powder X-ray diffraction (XRD) patterns were collected on a X-ray diffractometer (Rigaku D/Max2550VB+/PC, Cu Kα, λ = 1.5406 Å, 40 kV and 100 mA). The scanning electron microscope (SEM) images were observed on a FEI Quanta 200 environmental scanning electron microscope. Transmission electron microscope (TEM) was performed on a FEI Tecnai G2 F20 field TEM with the accelerating voltage of 200 kV. Energy-dispersive X-ray analysis (EDX) and the elemental mappings were carried out on an AMETEK Materials Analysis EDX equipped on the SEM and TEM. The materials were dispersed and loaded on the carbon-coated copper grids for TEM measurement. The atomic ratio of Co:Mg was determined by EDX and inductively coupled plasma optical emission spectrometry (ICP-OES, Aglient 5110). The X-ray photoelectron spectroscopy (XPS) analysis were analyzed on a Kratos AXIS ULTRA XPS equipped with a monochromatic Al Kα X-ray source (486.6 eV). Corrections of the binding energy were carried out using C 1s peak at 284.6 eV. The Raman spectra were measured on a Renishaw inVia confocal Raman microscope with the excitation laser line at 532 nm. The N_2 gas sorption isotherm and BET surface areas of the samples were obtained on a Micromeritics ASAP 2020. The contact angles were measured by a video-based contact angle instrument (OCA 20, Dataphysics).

Electrochemical characterization

Electrochemical measurements were performed on the CHI 660E electrochemical workstation at room temperature. Linear sweep voltammograms (LSV) and cyclic

voltammograms (CV) were measured in a standard three-electrode system with a glassy carbon (GC, 0.07 cm^2) electrode as the working electrode, saturated Ag/AgCl as the reference electrode, and graphite rod as the counter electrode. The working electrode was prepared as follows: 4 mg of the sample and 30 μL of Nafion was dispersed in a 1 mL of DI water solution, and then sonicated for 30 min to form a uniform suspension. 6 μL of well-dispersed ink was coated onto the GC electrode. The LSV and CV curves were recorded in a 1.0 M KOH solution with iR compensation (scan rates were 50 mV/s). The potentials were reported against to the reversible hydrogen electrode (RHE) with the following equation: $E_{RHE} = E_{Ag/AgCl} + (0.197 + 0.0591 \times pH)$ V. Tafel plots were obtained by measuring LSV with a scan rate of 2 mV/s. The controlled potential electrolysis (CPE) test was measured on indium tin oxide (ITO, 0.25 cm^2) electrode at 1.66 V without iR compensation. The electrochemical impedance spectroscopy (EIS) was recorded under different potentials from 0.01 Hz to 100000 Hz at the amplitude of the sinusoidal voltage of 5 mV.

Laviron equation

$$E_c = E_{1/2} - (RT/\alpha nF) \times \ln(\alpha nF/RTk_s) - (RT/\alpha nF) \times \ln \nu$$

In this equation, k_s is the rate constant of metal redox, ν is the scan rate, E_c is the reduction potential of metal redox, $E_{1/2}$ is the formal potential of metal redox, n and α are the number of electrons transferred and the transfer coefficient, respectively.

The surface coverage of intermediates could be calculated by the equation:

$$\theta(E) = \frac{1}{\sigma}\int_{E_0}^{E} C_a(E)\mathrm{d}E$$

In this equation, θ is the surface coverage of intermediate, σ is the charge density for the monolayer coverage, E_0 is the potential where intermediate adsorption occurs.

The possible OER mechanisms of Co-based catalysts:

$$Co^{2+} + 3OH^- \leftrightarrow CoOOH + H_2O + e^-$$
$$CoOOH + OH^- \leftrightarrow CoO_2 + H_2O + e^-$$
$$CoO_2 \rightarrow Co^{2+} + O_2 + 2e^-$$

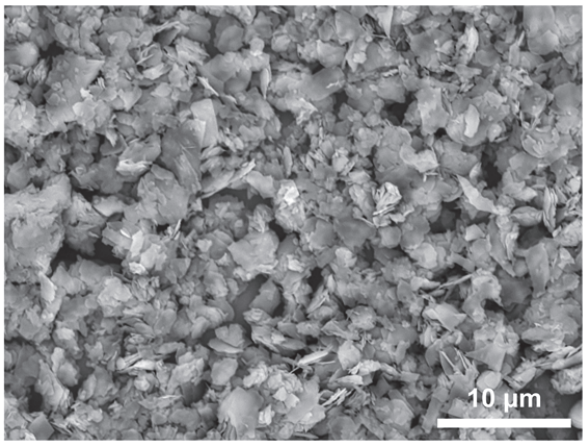

Fig. S1 The SEM image of the NH_4CoPO_4 precursor.

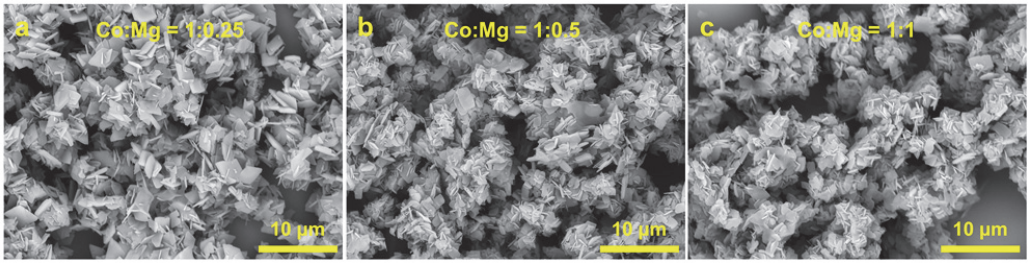

Fig. S2 The SEM images of the Mg-doped $Co_3(PO_4)_2$ materials prepared with different starting amounts of $MgCl_2$ (amounts are denoted in the images).

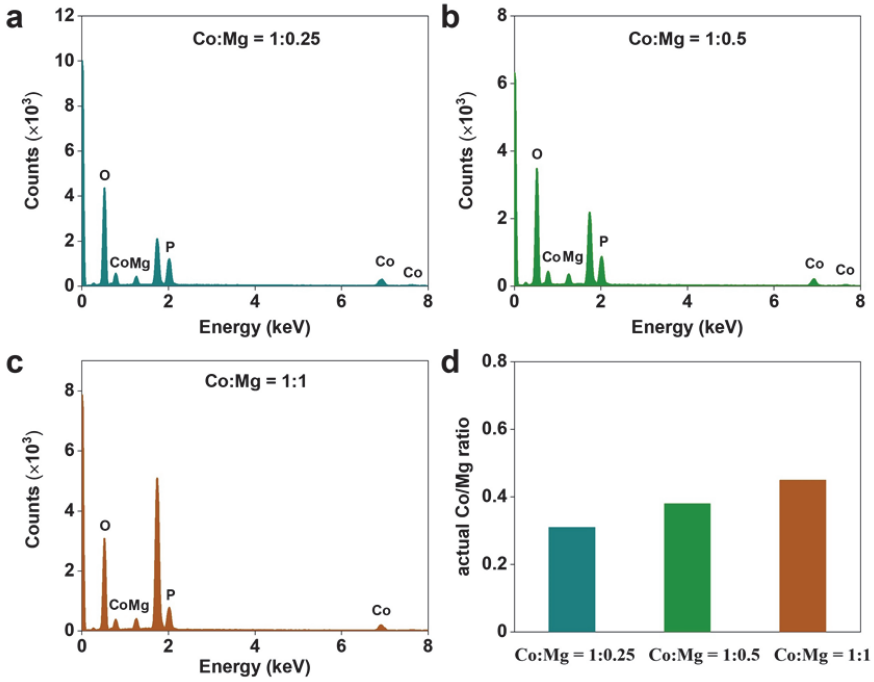

Fig. S3 (a-c) The EDX spectra of the Mg-doped $Co_3(PO_4)_2$ materials prepared with different starting amounts of $MgCl_2$ (amounts are denoted in the images). (d) The actual molar ratios of Co:Mg of the Mg-doped $Co_3(PO_4)_2$ materials from EDX measurements.

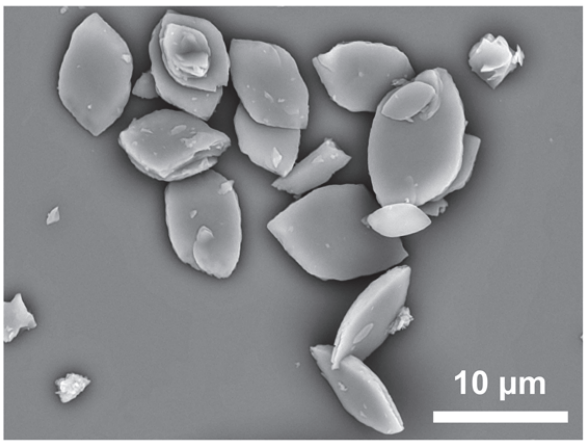

Fig. S4 The SEM image of pure $Co_3(PO_4)_2$ sample.

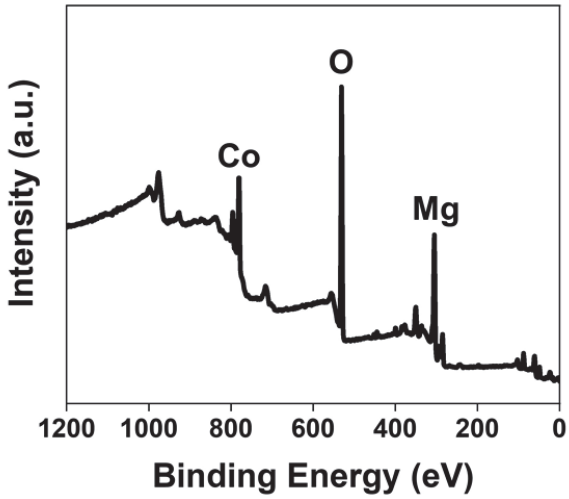

Fig. S5 The XPS spectrum of the Mg-doped $Co_3(PO_4)_2$ sample after 2 h of OER electrolysis at 1.66 V.

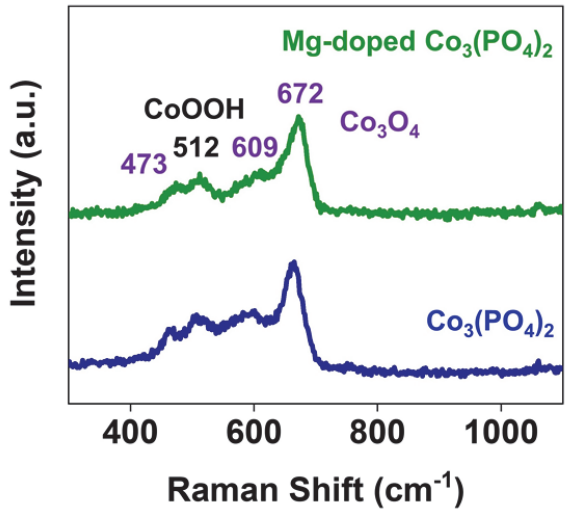

Fig. S6 The Raman spectra of the Mg-doped $Co_3(PO_4)_2$ and $Co_3(PO_4)_2$ samples after 2 h of OER electrolysis at 1.66 V. The Raman peaks at 473, 609 and 672 cm^{-1} are from E_g, F_{2g}, and A_{1g} modes of Co_3O_4, and the peak at 512 cm^{-1} is from CoOOH.[1]

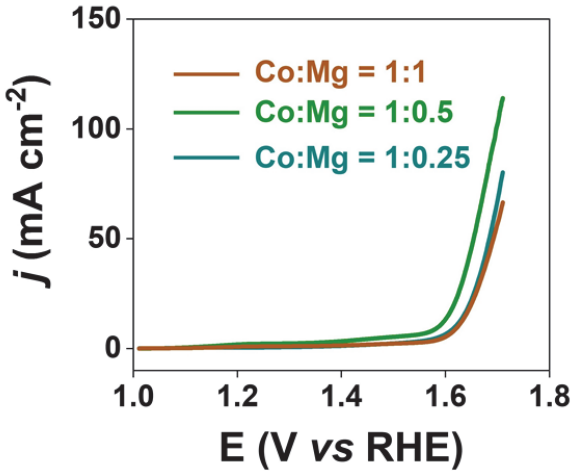

Fig. S7 The LSV curves of the samples prepared with different starting amounts of $MgCl_2$ for the OER.

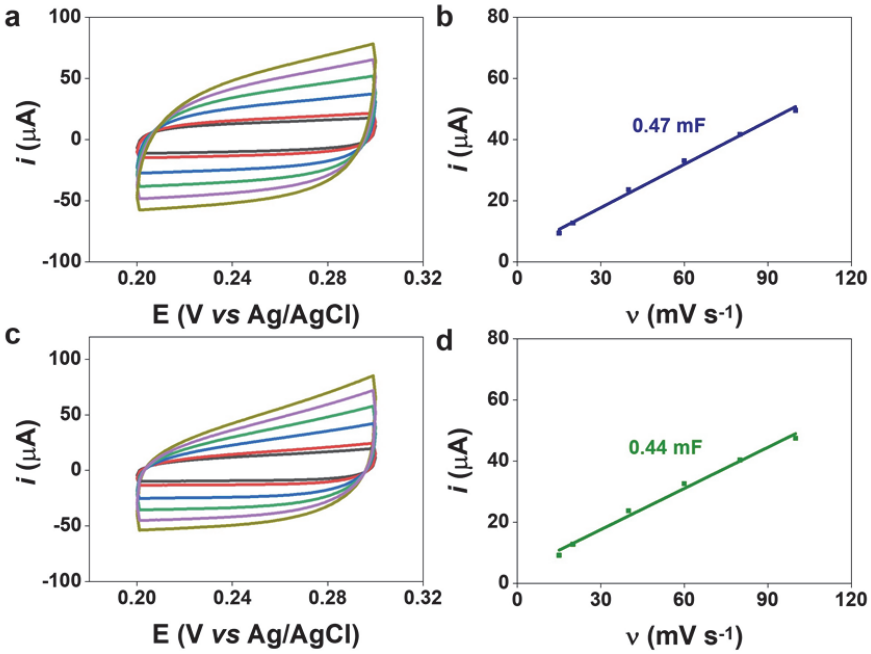

Fig. S8 The charging currents of (a) $Co_3(PO_4)_2$ and (c) Mg-doped $Co_3(PO_4)_2$ samples recorded in the non-Faradaic potential region at different scan rates (100 mV s^{-1}, 80 mV s^{-1}, 60 mV s^{-1}, 40 mV s^{-1}, 20 mV s^{-1}, 15 mV s^{-1}, from bottom to top). The anodic charging current at 0.25 V plotted against the scan rates, the slopes of which are capacitance values of (b) $Co_3(PO_4)_2$ and (d) Mg-doped $Co_3(PO_4)_2$ samples.

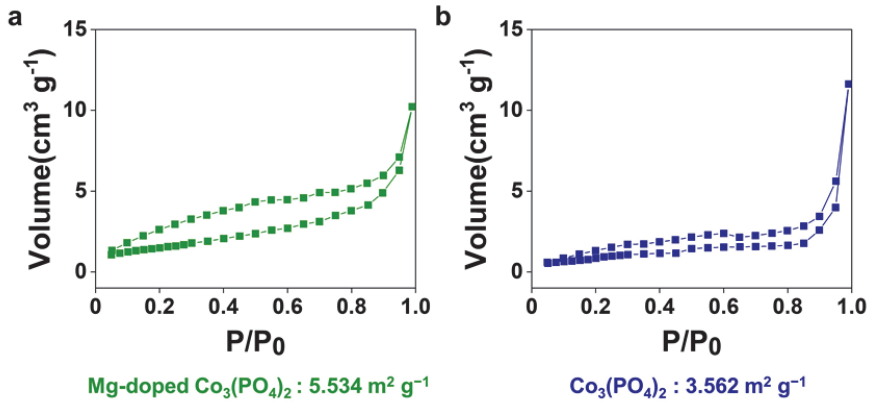

Fig. S9 The N_2 adsorption-desorption isotherms of (a) Mg-doped $Co_3(PO_4)_2$ and (b) $Co_3(PO_4)_2$ samples.

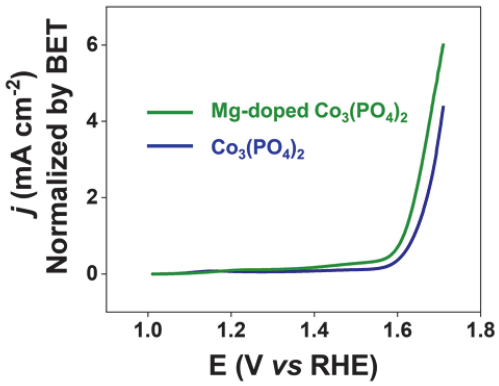

Fig. S10 The normalized OER currents by BET surface areas of Mg-doped $Co_3(PO_4)_2$ and $Co_3(PO_4)_2$ samples.

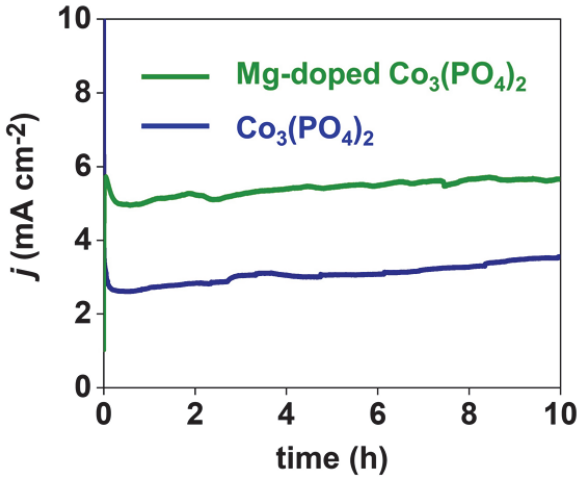

Fig. S11 The CPE curves of the Mg-doped $Co_3(PO_4)_2$ and $Co_3(PO_4)_2$ samples at 1.66 V without iR compensation.

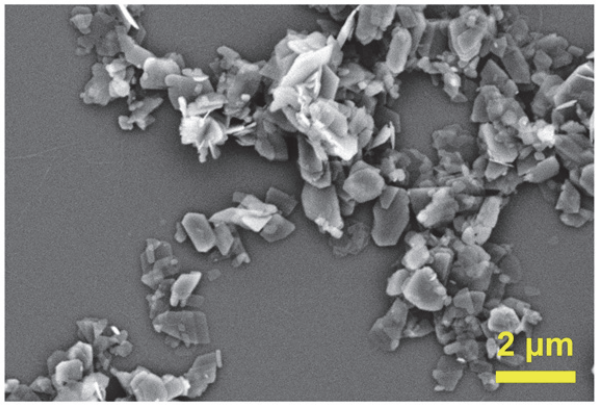

Fig. S12 The SEM image of the Mg-doped $Co_3(PO_4)_2$ after 2 h of electrolysis at 1.66 V. The result indicates Mg-doped $Co_3(PO_4)_2$ retains 2D structure after OER.

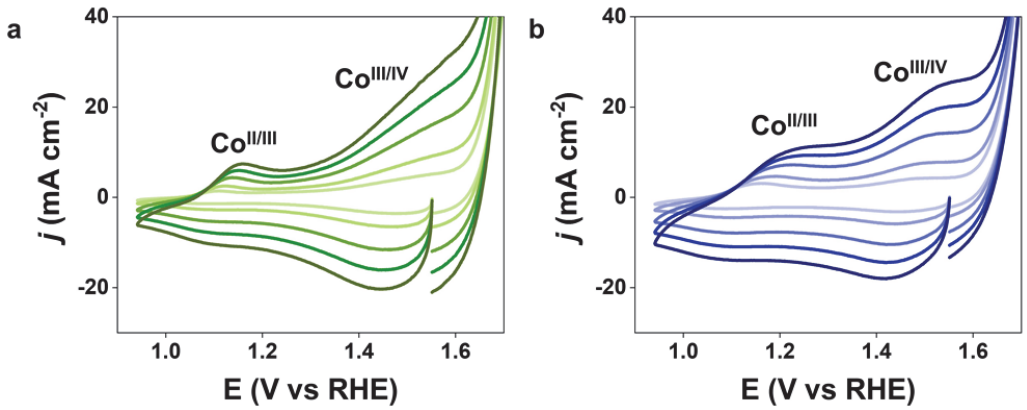

Fig. S13 CVs of (a) Mg-doped $Co_3(PO_4)_2$ and (b) $Co_3(PO_4)_2$ samples at scan rates of 0.5, 1, 2, 3 and 4 V s^{-1} (increasing capacitive currents) in 1.0 M KOH solutions.

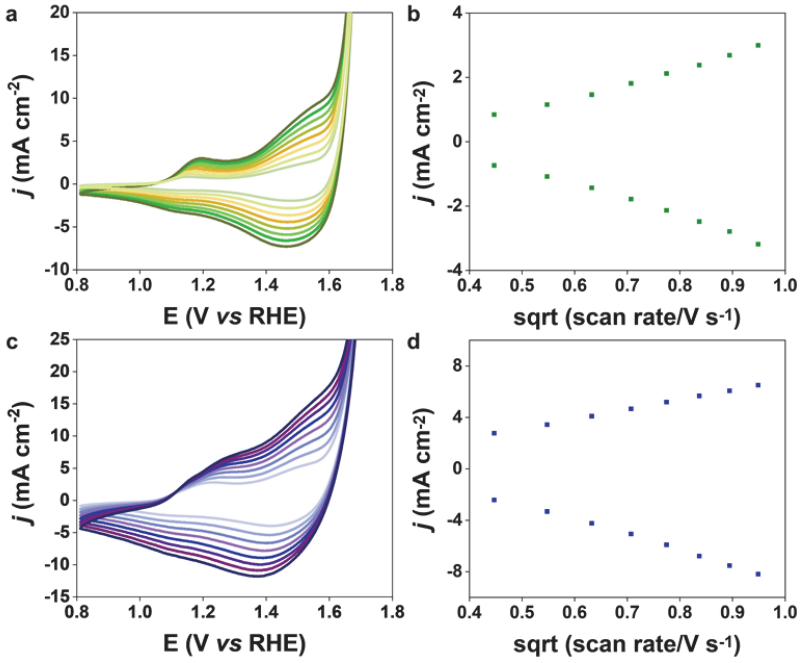

Fig. S14 CVs of (a) Mg-doped $Co_3(PO_4)_2$ and (c) $Co_3(PO_4)_2$ with scan rates from 0.2 to 0.9 V s^{-1}. The plot of the redox peak currents densities versus the square root of scan rates of (b) Mg-doped $Co_3(PO_4)_2$ and (d) $Co_3(PO_4)_2$.

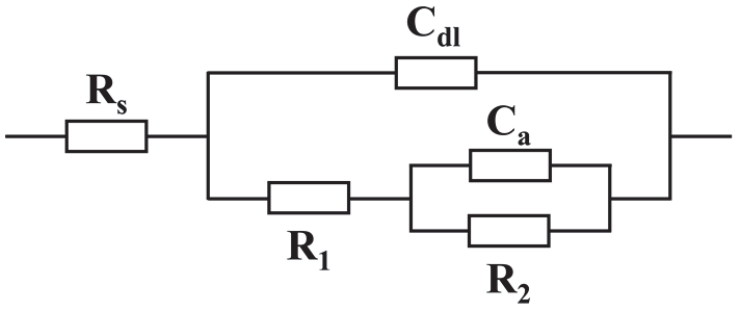

Fig. S15 The electrical equivalent circuit of the Mg-doped $Co_3(PO_4)_2$ and $Co_3(PO_4)_2$ materials.

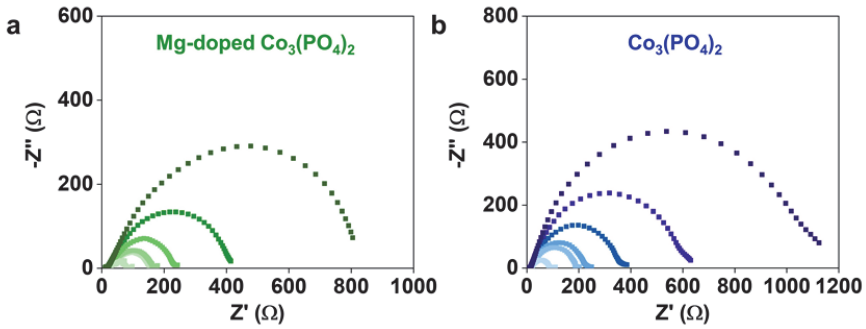

Fig. S16 Nyquist plots of (a) Mg-doped $Co_3(PO_4)_2$ and (b) $Co_3(PO_4)_2$ at different applied potentials (1.66 V, 1.61 V, 1.60 V, 1.58 V, 1.56 V, 1.54 V, from bottom to top). Cobalt phosphate materials exhibit p-type semiconductor properties, which possess poor intrinsic electrical conductivity.[2,3]

References

1 B. S. Yeo and A. T. Bell, *J. Am. Chem. Soc.*, 2011, **133**, 5587-5593.

2 C. Costentin, T. R. Porter and J.-M. Savéant, *J. Am. Chem. Soc.*, 2016, **138**, 5615-5622.

3 T. Zhou, Y. Du, D. Wang, S. Yin, W. Tu, Z. Chen, A. Borgna and R. Xu, *ACS Catal.*, 2017, **7**, 6000-6007.